Sussex Research Online

Active terahertz two-wire waveguides

Article (Published Version)

Mridha, Manoj Kumar, Mazhorova, Anna, Clerici, Matten, Al-Naib, Ibraheem, Daneau, Maxime, Ropagnol, Xavier, Peccianti, Marco, Reimer, Christian, Ferrera, Marcello, Razzari, Luca, Vidal, Francois and Morandotti, Roberto (2014) Active terahertz two-wire waveguides. Optics Express, 22 (19). pp. 22340-22348. ISSN 1094-4087

This version is available from Sussex Research Online: http://sro.sussex.ac.uk/id/eprint/55750/

This document is made available in accordance with publisher policies and may differ from the published version or from the version of record. If you wish to cite this item you are advised to consult the publisher's version. Please see the URL above for details on accessing the published version.

Copyright and reuse:
Sussex Research Online is a digital repository of the research output of the University.

Copyright and all moral rights to the version of the paper presented here belong to the individual author(s) and/or other copyright owners. To the extent reasonable and practicable, the material made available in SRO has been checked for eligibility before being made available.

Copies of full text items generally can be reproduced, displayed or performed and given to third parties in any format or medium for personal research or study, educational, or not-for-profit purposes without prior permission or charge, provided that the authors, title and full bibliographic details are credited, a hyperlink and/or URL is given for the original metadata page and the content is not changed in any way.

http://sro.sussex.ac.uk

Active terahertz two-wire waveguides

Manoj Kumar Mridha,[1] Anna Mazhorova,[1] Matteo Clerici,[1,2,*] Ibraheem Al-Naib,[3] Maxime Daneau,[1] Xavier Ropagnol,[1] Marco Peccianti,[4] Christian Reimer,[1] Marcello Ferrera,[2] Luca Razzari,[1] François Vidal,[1] and Roberto Morandotti[1]

[1]INRS-Énergie, Matériaux et Télécommunications, Varennes, Québec J3X 1S2, Canada
[2]School of Engineering and Physical Sciences, Heriot-Watt University, Edinburgh EH14 4AS, UK
[3]Department of Physics, Engineering Physics and Astronomy, Queen's University, Kingston K7L 3N6, Canada
[4]Dept. of Physics and Astronomy, University of Sussex, Falmer, Brighton BN1 9QH, UK
**m.clerici@hw.ac.uk*

Abstract: We demonstrate, by generating a THz electric field directly within the guiding structure, an active two-wire waveguide operating in the terahertz (THz) range of wavelengths. We compare the energy throughput of the active configuration with that of a radiatively coupled semi-large photoconductive antenna, in which the radiation is generated outside the waveguide, reporting a 60 times higher energy throughput for the same illumination power and applied voltage. This novel, active waveguide design allows to have efficient coupling of the THz radiation in a dispersion-less waveguide without the need of involved radiative coupling geometries.

©2014 Optical Society of America

OCIS codes: (300.6495) Spectroscopy, terahertz; (230.7370) Waveguides; (350.2770) Gratings.

References and links

1. S. P. Jamison, R. W. Mc Gowan, and D. Grischkowsky, "Single-mode waveguide propagation and reshaping of sub-ps terahertz pulses in sapphire fibers," Appl. Phys. Lett. **76**(15), 1987–1989 (2000).
2. R. Mendis and D. Grischkowsky, "Plastic ribbon THz waveguides," J. Appl. Phys. **88**(7), 4449–4451 (2000).
3. M. Rozé, B. Ung, A. Mazhorova, M. Walther, and M. Skorobogatiy, "Suspended core subwavelength fibers: towards practical designs for low-loss terahertz guidance," Opt. Express **19**(10), 9127–9138 (2011).
4. L.-J. Chen, H.-W. Chen, T.-F. Kao, J.-Y. Lu, and C.-K. Sun, "Low-loss subwavelength plastic fiber for terahertz waveguiding," Opt. Lett. **31**(3), 308–310 (2006).
5. S. Atakaramians, S. Afshar V, T. M. Monro, and D. Abbott, "Terahertz dielectric waveguides," Adv. Opt. Photon. **5**(2), 169–215 (2013).
6. K. Wang and D. M. Mittleman, "Metal wires for terahertz wave guiding," Nature **432**(7015), 376–379 (2004).
7. T.-I. Jeon, J. Zhang, and D. Grischkowsky, "THz Sommerfeld wave propagation on a single metal wire," Appl. Phys. Lett. **86**(16), 161904 (2005).
8. R. Mendis and D. Grischkowsky, "THz interconnect with low-loss and low-group velocity dispersion," IEEE Microw. Wirel. Compon. Lett. **11**(11), 444–446 (2001).
9. M. Mbonye, R. Mendis, and D. M. Mittleman, "A terahertz two-wire waveguide with low bending loss," Appl. Phys. Lett. **95**(23), 233506 (2009).
10. H. Pahlevaninezhad and T. E. Darcie, "Coupling of terahertz waves to a two-wire waveguide," Opt. Express **18**(22), 22614–22624 (2010).
11. H. Pahlevaninezhad, T. E. Darcie, and B. Heshmat, "Two-wire waveguide for terahertz," Opt. Express **18**(7), 7415–7420 (2010).
12. P. Tannouri, M. Peccianti, P. L. Lavertu, F. Vidal, and R. Morandotti, "Quasi-TEM mode propagation in twin-wire THz waveguides," Chin. Opt. Lett. **9**, 110013 (2011).
13. J. A. Deibel, K. Wang, M. D. Escarra, and D. Mittleman, "Enhanced coupling of terahertz radiation to cylindrical wire waveguides," Opt. Express **14**(1), 279–290 (2006).
14. J. Anthony, R. Leonhardt, and A. Argyros, "Hybrid hollow core fibers with embedded wires as THz waveguides," Opt. Express **21**(3), 2903–2912 (2013).
15. A. Markov and M. Skorobogatiy, "Two-wire terahertz fibers with porous dielectric support," Opt. Express **21**(10), 12728–12743 (2013).
16. M. K. Mridha, A. Mazhorova, M. Daneau, M. Clerici, M. Peccianti, P.-L. Lavertu, X. Ropagnol, F. Vidal, and R. Morandotti, "Low dispersion propagation of broadband THz pulses in a two-wire waveguide," *Conference on Lasers and Electro-Optics*, Technical Digest (CD) (Optical Society of America, 2013), paper. CTh1K.6.

#213416 - $15.00 USD Received 3 Jun 2014; revised 12 Aug 2014; accepted 21 Aug 2014; published 8 Sep 2014

17. P. R. Smith, D. H. Auston, and M. C. Nuss, "Subpicosecond photoconducting dipole antennas," IEEE J. Quantum Electron. **24**(2), 255–260 (1988).
18. G. Zhao, R. N. Schouten, N. van der Valk, W. T. Wenckebach, and P. C. M. Planken, "Design and performance of a THz emission and detection setup based on a semi-insulating GaAs emitter," Rev. Sci. Instrum. **73**(4), 1715–1719 (2002).
19. S. Preu, G. H. Döhler, S. Malzer, L. J. Wang, and A. C. Gossard, "Tunable, continuous-wave Terahertz photomixer sources and applications," J. Appl. Phys. **109**(6), 061301 (2011).
20. M. R. Stone, M. Naftaly, R. E. Miles, J. R. Fletcher, and D. P. Steenson, "Electrical and radiation characteristics of semilarge photoconductive terahertz emitters," IEEE T. Microw. Theory **52**(10), 2420–2429 (2004).
21. Q. Wu, M. Litz, and X. C. Zhang, "Broadband detection capability of ZnTe electro-optic field detectors," Appl. Phys. Lett. **68**(21), 2924–2926 (1996).
22. A. Tomasino, A. Parisi, S. Stivala, P. Livreri, A. C. Cino, A. C. Busacca, M. Peccianti, and R. Morandotti, "Wideband THz time domain spectroscopy based on optical rectification and electro-optic sampling," Sci Rep **3**, 3116 (2013).
23. P. Petruzzi, C. Lowry, and P. Sivanesan, "Dispersion compensation using only fiber Bragg gratings," IEEE J. Sel. Top. Quantum Electron. **5**(5), 1339–1344 (1999).
24. A. M. Vengsarkar, P. J. Lemaire, J. B. Judkins, V. Bhatia, T. Erdogan, and J. E. Sipe, "Long-period fiber gratings as band-rejection filters," J. Lightwave Technol. **14**(1), 58–65 (1996).
25. K. O. Hill, B. Malo, F. Bilodeau, S. Thériault, D. C. Johnson, and J. Albert, "Variable-spectral-response optical waveguide Bragg grating filters for optical signal processing," Opt. Lett. **20**(12), 1438–1440 (1995).
26. I. Baumann, J. Seifert, W. Nowak, and M. Sauer, "Compact all-fiber add-drop-multiplexer using fiber Bragg gratings," IEEE Photon. Technol. Lett. **8**(10), 1331–1333 (1996).
27. L. Wentai, Z. Chunxi, L. Lijing, and L. Sheng, "Review on development and applications of fiber-optic sensors," in *Symposium on Photonics and Optoelectronics (SOPO), 2012*, pp. 1–4.
28. A. Farhad, "Fiber optic health monitoring of civil structures using long gage and acoustic sensors," Smart Mater. Struct. **14**(3), S1–S7 (2005).
29. G. Yan, A. Markov, Y. Chinifooroshan, S. M. Tripathi, W. J. Bock, and M. Skorobogatiy, "Low-loss terahertz waveguide Bragg grating using a two-wire waveguide and a paper grating," Opt. Lett. **38**(16), 3089–3092 (2013).
30. S. F. Zhou, L. Reekie, H. P. Chan, K. M. Luk, and Y. T. Chow, "Terahertz filter with tailored passband using multiple phase shifted fiber Bragg gratings," Opt. Lett. **38**(3), 260–262 (2013).
31. Lumerical Solutions, Inc., https://*www.lumerical.com/tcad-products/fdtd/*.
32. Y.-S. Jin, G.-J. Kim, and S.-G. Jeon, "Terahertz dielectric properties of polymers," J. Korean Phys. Soc. **49**, 513–517 (2006).

1. Introduction

The development of waveguides with low dispersion propagation of broadband terahertz (THz) pulses is essential to realize interconnects for future THz communication networks, enhanced THz-time domain spectroscopy (TDS), and to develop new sensing technologies. To date, several THz waveguides have been reported based on dielectric and metallic structures. On the one hand, dielectric based waveguides such as sapphire fibers [1], plastic ribbon waveguides [2] and sub-wavelength fibers [3, 4] are not suitable for low dispersion propagation of THz pulses due to the inherent dispersive properties and losses at frequencies above 1 THz. Although hollow core dielectric fibers can boost low-loss and low-dispersion, they are limited in bandwidth due to resonances or bandgap effects [5]. On the other hand, metallic waveguides such as single wire waveguides [6, 7], parallel plate waveguides [8] and two-wire waveguides [9–12] support the propagation of single cycle THz pulses with low dispersion due to their (almost) non-dispersive transverse electromagnetic mode (TEM). Single wire waveguides carrying radially polarized TEM modes are difficult to excite from commonly available linearly polarized THz sources – such as photoconductive (PC) antennas - due to mode mismatch, and hence it is necessary to make use of a radially polarized THz radiation source [13]. Furthermore, single-wire waveguides are featured by high bending losses, which limit the flexibility of such a solution. Although the low dispersion modes of PPWGs can be conveniently excited by a commonly available PC antenna, such waveguides cannot be used for long propagation distances. This is due to the one dimensional THz confinement in these waveguides which leads to beam expansion in the unguided dimension, and hence subsequent loss due to diffraction. The linearly polarized TEM mode of a two-wire waveguide can be easily excited via a PC antenna and is featured by low bending losses - in contrast to single wire waveguides [9]. In addition, a two-wire waveguide provides a tight

#213416 - $15.00 USD Received 3 Jun 2014; revised 12 Aug 2014; accepted 21 Aug 2014; published 8 Sep 2014
(C) 2014 OSA

two-dimensional confinement of the TEM mode and can thus be employed for guiding over longer distances.

Recently, a metal-dielectric air-core fiber with two embedded indium wires [14] and a two-wire waveguide structure supported by porous dielectric fibers [15] have been demonstrated experimentally and theoretically, respectively. The unique ability of the two-wire waveguide to carry a tightly confined linearly polarized TEM mode makes it very promising for future THz interconnects and opens up new prospects for short range ultra-broadband telecommunication networks. One issue that still needs to be addressed is how to efficiently couple THz pulses into the two-wire guiding structure. Both the TEM mode supported by a two-wire waveguide and the THz radiation generated by a PC antenna are linearly polarized. The combined system consisting of a PC antenna interconnected with a two-wire waveguide will therefore be a very effective solution for the efficient generation, coupling and routing of the THz signal. In earlier works [9, 16], the two-wire waveguide mode was excited by positioning a PC antenna close to the input of the waveguide. In this configuration, it can be assumed that the THz radiation is being coupled into the waveguide from free space, similar to the coupling demonstrated numerically in [10] by considering a single dipole source. However, a large fraction of this free space THz radiation, emitted by the PC antenna, is not coupled into the waveguide and the low, far-field mediated coupling efficiency of the system strongly limits its applicability. The main limiting factor is the difficulty of focusing the THz radiation at the input of the two-wire waveguide as the size of the gap between the wires is close to the diffraction limit.

In this work we address this issue by generating the THz radiation directly inside the waveguide (i.e. active wave-guiding). This is achieved by shining a short laser pulse on a thin piece of GaAs inserted between the wires under a given voltage, following the principle at the basis of a (semi-) large area photoconductive antenna [17–20]. We compare the energy throughput of the active waveguide configuration with that obtained by a semi-large area photoconductive antenna, driven by the same potential, illuminated by the same optical power and consisting of the same semiconductor sample. We also compare the active waveguide throughput with that obtained by placing the semi-large area PC antenna in close proximity to the 10 cm waveguide, so that radiative coupling can occur between the emitted and the guided mode. We note that these comparisons are only meant to provide an overview of the advantage of the active configuration proposed. No optimization of the radiative coupling between the semi-large PC antenna and the waveguide has been attempted.

2. Two-wire THz transmitter

The design of the fabricated active two-wire waveguide is based on the passive waveguide structure reported in [16], where the low-dispersion and broadband nature of this configuration was demonstrated for a wire separation of 300 μm. Figures 1(a) and 1(b) show photographs of the 10 cm long waveguide used to build the active waveguide and a detail of its input end, respectively. From here on, we shall refer to the resulting active waveguide as a *two-wire THz transmitter* (TWT). The TWT consists of a piece of GaAs highlighted in Fig.1(b), held between the wires of the waveguide, which is supported by an aluminum base plate acting as its backbone.

#213416 - $15.00 USD Received 3 Jun 2014; revised 12 Aug 2014; accepted 21 Aug 2014; published 8 Sep 2014
(C) 2014 OSA

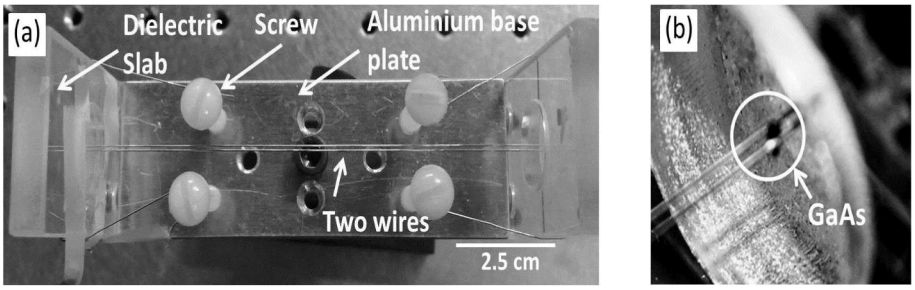

Fig. 1. (a) 10 cm long two-wire transmitter in a passive configuration. The wires are held under tension by wrapping them around plastic screws. An aluminum base plate supports the two-wire waveguide design. (b) A thin GaAs piece (300 μm × 300 μm × 5mm) inserted between the wires and serving as a semi-large area PC antenna inside the *two-wire THz transmitter* (active configuration).

Two dielectric slabs are then attached to either ends of the base plate. The dielectric slabs have an 800 μm diameter hole drilled through their centres [Fig. 2(a)]. As shown in the figure, each of the two copper wires (diameter = 250 μm) pass through the centre of these holes on either side of the base plate. As the diameter of the hole is 800 μm, a space of 300 μm is left between the two wires. In order to maintain a uniform separation between the wires, they are kept under tension. Such tension is applied by wrapping the four free ends of the wires around a set of screws [Fig. 1(a)]. Finally, a thin rectangular piece of GaAs (300 μm × 300 μm × 5 mm) is inserted between the two wires to form the TWT as shown in Fig. 1(b). The electric field required for activating the integrated semi-large area PC antenna is obtained by applying a voltage directly to the copper wires. Hence, to avoid a short circuit in the system, the screws were made of plastic. In order to increase the contact efficiency between the copper wires and the GaAs piece, silver paint was applied at the contact points.

The TWT supports a linearly polarized, tightly confined TEM mode at 1 THz. A theoretical study [12] has shown that with the increase in wire separation, the mode carried by the two-wire waveguide is no longer linearly polarized as it breaks down to two weakly coupled Sommerfeld modes (radially polarized modes). Hence in order for a two-wire waveguide to carry a linear polarization, the separation between the two wires needs to be very close to the wavelength of operation. In this work, we employed a wire separation of S = 300 μm so that the waveguide is suitable for carrying THz radiation with a central wavelength of λ = 300 μm (corresponds to 1 THz in frequency).

3. Results and discussions

3.1 Active and passive waveguide configurations

We compared the energy throughput for the passive configuration (THz semi-large area PC antenna; two-wire waveguide; detection) with the TWT (active two-wire waveguide; detection) at constant optical excitation power and applied potential. To this end we carried out three experiments employing an electro-optical sampling setup for THz detection. In the first experiment no waveguide was used. The purpose of the first measure was to record the THz pulse from a PC antenna, so that its THz pulse energy can be used as a reference to evaluate the coupling efficiency of the passive and active waveguide configuration. A scheme of this experiment is reported in Fig. 2(b). A thin rectangular piece of GaAs is held between two copper strips serving as electrodes [see Fig. 2(c)], so that when a bias voltage is applied, this configuration serves as a semi-large area PC antenna for THz generation. The emitted radiation is collimated by a parabolic mirror confocal to the emission point and, after proper

#213416 - $15.00 USD Received 3 Jun 2014; revised 12 Aug 2014; accepted 21 Aug 2014; published 8 Sep 2014
(C) 2014 OSA

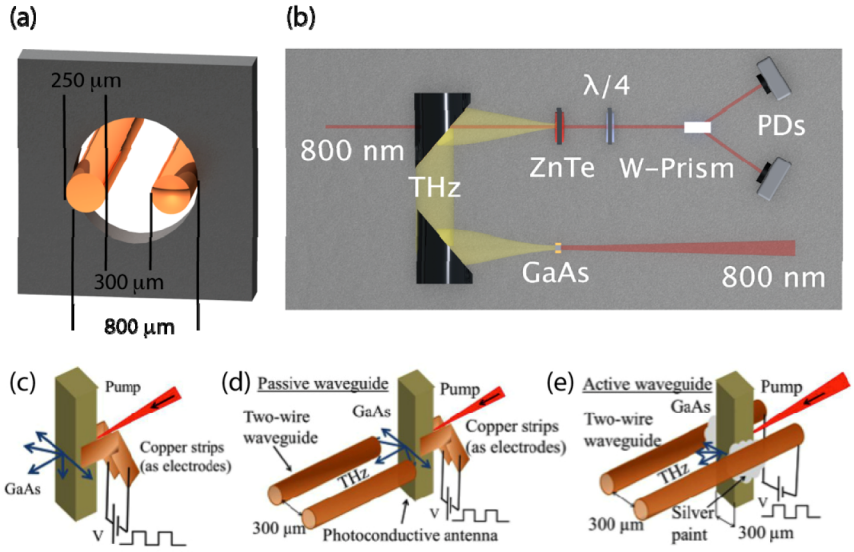

Fig. 2. (a) Schematic for the dielectric support holder for the wires of diameter 250 μm. The central hole is 800 μm in diameter, while the separation between the two wires is 300 μm. (b) Top-view of the experimental setup used for calibrating the maximum signal attainable from the GaAs integrated semi-large area PC antenna. The emitted THz radiation is focused onto a ZnTe crystal. Changes in the probe beam (800 nm) polarization are measured using a Wollaston prism and photo detectors (PDs). (c) Details of the integrated semi-large area PC antenna used to generate THz radiation, (d) schematic of the passive configuration where the THz radiation from the integrated semi-large area PC antenna is coupled into the two-wire waveguide, (e) schematic of the active configuration; here both the generation and the coupling of the THz radiation occur directly inside the two-wire waveguide. The arrows indicate the direction of the THz radiation emitted in each case in the plane containing the two wires.

filtering, is focused onto the detection crystal (Zinc Telluride - ZnTe) by a second parabolic mirror, collinearly with an 800 nm optical probe pulse. A balanced detection scheme allows to record the variation of the probe polarization induced by the THz field in the ZnTe crystal via the electro-optical effect as a function of the delay between the probe and the THz pulse, where the recorded signal is proportional to the THz electric field [21,22].

In a second experiment, we evaluated the coupling efficiency of the passive configuration. The same semi-large area PC antenna, external to the guiding structure, was coupled to the 10 cm length two-wire waveguide [passive configuration; Fig. 2(d)]. The THz pulse was measured after propagation through the waveguide, with the output of the waveguide focused on the first parabolic mirror of the detection scheme. We note that this configuration does not guarantee optimal coupling of the radiation emitted by the semi-large photoconductive antenna into the waveguide. To that end specific optimization strategies should be investigated, which elude the scope of this paper.

Finally, in the third experiment, the mode coupling of the THz pulse from the 10 cm long two-wire transmitter in the active configuration [Fig. 2(e)] was recorded. The waveguides used for the second and the third had the same dimensions (for the sake of comparison). Note that we employed the same GaAs piece in all three experiments.

In order to pump the THz Kit we used a Ti:Sapphire mode locked laser (Mai-Tai, Spectra-Physics) with 125 fs pulse duration and 80 MHz repetition rate. Electro-optical sampling has been performed in a [110] ZnTe crystal of 2 mm thickness, in order to characterize the THz signal. The copper wires are connected to a modulator, consisting of a bipolar high voltage source able to supply 110 V at 11 kHz.

#213416 - $15.00 USD Received 3 Jun 2014; revised 12 Aug 2014; accepted 21 Aug 2014; published 8 Sep 2014
(C) 2014 OSA

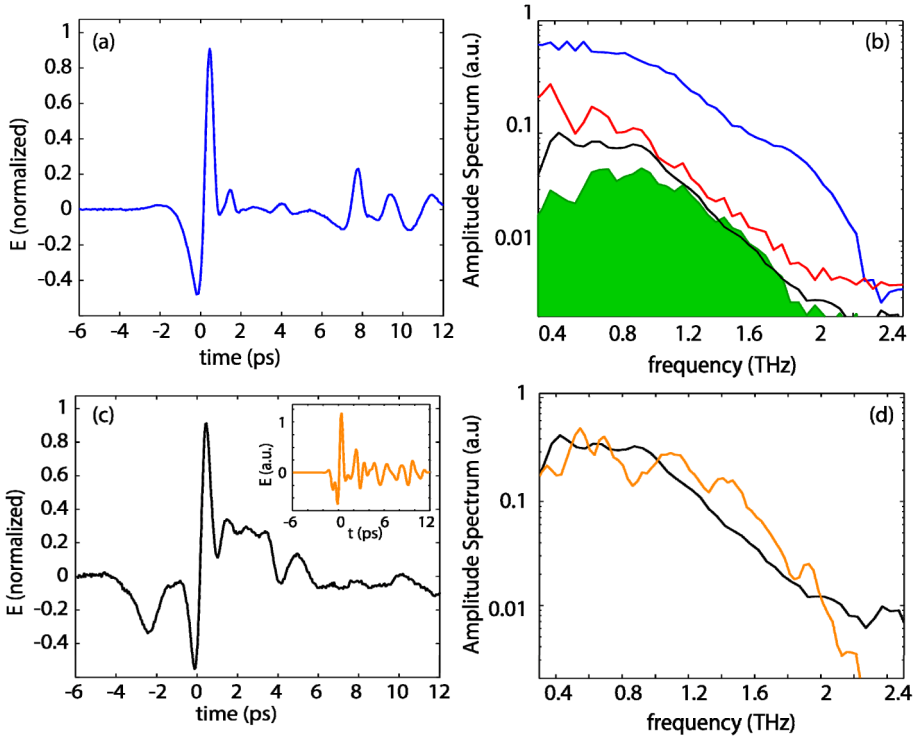

Fig. 3. (a) Measured temporal waveform from the GaAs piece used as a PC antenna (normalized to its peak). (b) Measured power spectra of the PC antenna (blue), 10 cm waveguide (green), 10 cm long TWT (red) and 20 cm long TWT (black), normalized to the peak of the semi-large area PC antenna's spectrum. (c) Measured THz waveform of the 20 cm long TWT (normalized to its peak). In the inset, simulated THz waveform emitted by the 20 cm TWT. (d) Comparison between the numerical and experimental spectra recorded at the output of the 20 cm long TWT.

3.2 Comparison of energy throughputs

Figure 3(a) shows the reference THz waveform as emitted by the semi-large area PC antenna [Fig. 2(c)], normalized to its peak. We note that here reflections occur both in the detection and in the generation side of our experiment, an issue that we are currently addressing. The measured power spectra of the semi-large area PC antenna (blue curve) and of the signals obtained from both waveguide configurations, namely passive two-wire waveguide (green shaded) and TWT (red for a 10 cm long WG and black for a 20 cm long WG) are presented in Fig. 3(b).

The energy of the output pulses, normalized to the energy of the PC antenna was extracted by integrating the square of their measured temporal field profile. We found that the pulse energy for the 10 cm long waveguide and TWT were nearly 0.6% and 40% of the pulse energy of the PC antenna, respectively, showing that the TWT couples a THz signal 60 times stronger than that achieved by approaching the semi-large area PC antenna to the waveguide.

In order to estimate the propagation losses of our TWTs, we compared the normalized output energy of the 10 cm long TWT with a 20 cm long equivalent structure, and found that the additional 10 cm of waveguide added ~11 dB of loss. Figure 3(c) shows the output waveforms for the 20 cm long TWT (normalized to its peak). We note that the 20 cm waveguide has not been optimized in all its parameters, for instance in terms of uniformity of the separation between the copper wires. Yet at this stage we only wish to demonstrate that

#213416 - $15.00 USD Received 3 Jun 2014; revised 12 Aug 2014; accepted 21 Aug 2014; published 8 Sep 2014
(C) 2014 OSA

single cycle pulses can be generated and transported by the proposed configuration and that the spectrum is not significantly different with respect to the 10 cm long case.

We numerically investigated the 20 cm active waveguide case and we show in Fig. 3(d) the comparison between the spectrum of the simulated pulse (orange) and that of the experimentally recorded electric field (black). In the inset of Fig. 3(c) we present the simulated time dependent electric field. The comparison shows a quite good agreement between our numerical simulation and the experimental results. For the numerical evaluation of the 20 cm long TWT's signal, a commercial package (CST Microwave Studio) has been employed and perfectly matched layer boundary conditions have been used with "open-add space" boundary conditions applied in all directions. The simulation environment mimics the experimental configuration with a photoexcitation signal of 120 fs duration, which determines the rise time of the photocurrent in GaAs. Subsequently, free carriers are generated in the substrate and hence the decay time depends on the carrier lifetime of the photoconductive material. The GaAs wafer is considered to be lossless and dispersionless and the copper wires are completely homogenous. The discrepancy between the experimental results and simulated data can be ascribed to inhomogeneity in the wires along the waveguide and accompanying losses and scattering.

5. Conclusion

In conclusion, we have addressed the issue of coupling THz radiation efficiently in a passive two-wire waveguide by introducing a novel active waveguide design (named as a *two-wire THz transmitter*, TWT), in which the generation of the THz signal occurs directly inside the guiding structure. This was realized by inserting a small piece of GaAs in between the two wires of the waveguide, serving as a semi-large photoconductive antenna. The wires of the waveguide act as the electrodes of the device, connected to a modulator, consisting of a bipolar high voltage source able to supply 110 V at 11 kHz. We found that the pulse energy collected by our detection system for the 10 cm long passive waveguide is 40% of the pulse energy of the semi-large area photoconductive antenna when employing as emitter the same piece of semiconductor (for a given potential and illumination power). These results may be of interest for the development of future ultra-broad band short-range telecommunication networks.

APPENDIX

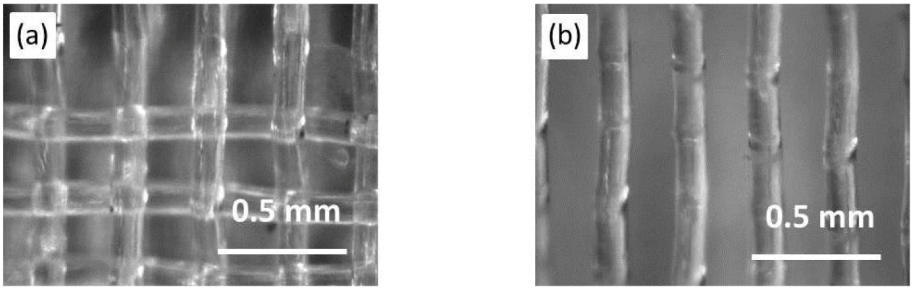

Fig. 4. (a) The actual polymer mesh with the horizontal and vertical rods. (b) The vertical polymer rods used for the experiment after removing the horizontal rods of the mesh. The average diameter of these rods, as measured under a microscope, is 110 ± 10 μm and the average air spacing in between the rods is 137 ± 20 μm. As a result the period of the grating is approximately 247 ± 30 μm.

As an example of application of the proposed two-wire waveguide, and in order to show the potential for a modular approach, we demonstrated "active" frequency filtering by inserting a polymer Bragg grating between the two wires. Bragg gratings are a key component of fiber optics based communication systems. They have been employed for dispersion compensation

#213416 - $15.00 USD Received 3 Jun 2014; revised 12 Aug 2014; accepted 21 Aug 2014; published 8 Sep 2014
(C) 2014 OSA

[23], the realization of band rejection filters [24], wavelength selective devices [25, 26], sensing [27], structural health monitoring [28] and other applications. Similarly, Bragg gratings can also be used to achieve THz frequency filtering [29, 30] which can find several applications in THz communication and spectroscopy.

For this work, we fabricated a Bragg grating from a low-cost polymer mesh made of extruded polypropylene. In the original polymer mesh shown in Fig. 4(a), horizontal and vertical sets of polymer rods are woven together. To obtain a one-dimensional structure for the grating, we removed the horizontal set of polymer rods from the mesh and used the vertical rods as the Bragg grating (Fig. 4(b)). The average diameter of these rods - as measured under an optical microscope - is 110 ± 10 μm and the average air spacing in between the rods is 137 ± 20 μm. As a result the period of the grating is approximately 247 ± 30 μm. For the proposed experiment, 16 periods of the grating were employed, approximately resulting in a 4 mm long sample.

The measured temporal signals are shown in Fig. 5(a). As it can be clearly seen, the peak amplitude of the signal is delayed due to the insertion of the grating, which increases the

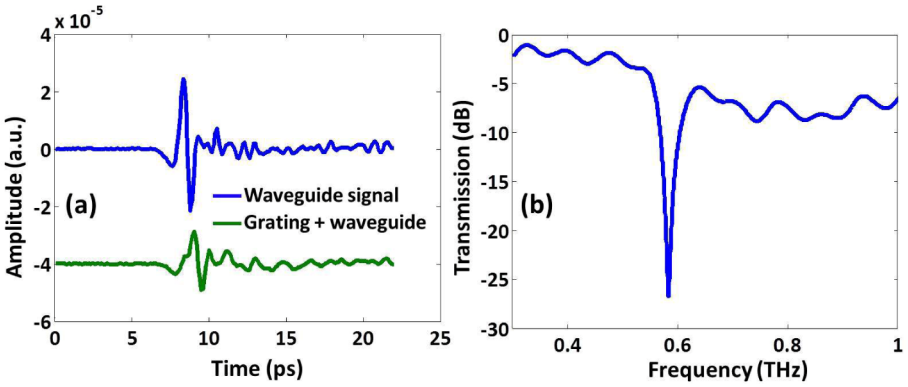

Fig. 5. (a) Measured temporal waveforms from the 10 cm TWT (in blue) and with the inserted grating (in green) (b) Transmission spectrum of the signal detected after inserting the grating in the waveguide. A fine notch of 23 dB is observed at 0.58 ± 0.01 THz with a line width of ~16 GHz.

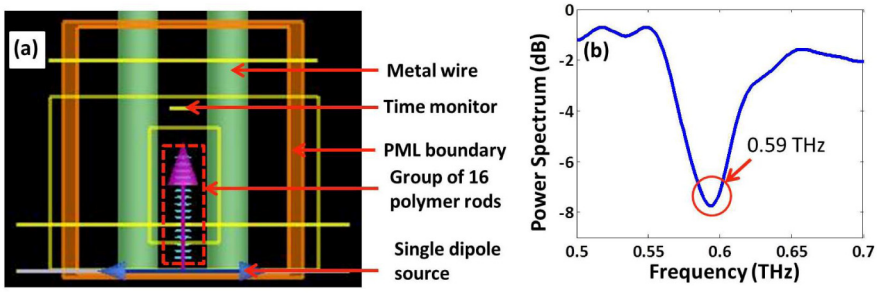

Fig. 6. (a) Snapshot of the FDTD simulation layout (top view) of the polymer Bragg grating inserted in the two-wire waveguide. A time monitor records the time varying electric field of the THz pulse (generated by the single dipole source) after passing through the Bragg grating. (b) Power spectrum of the grating response recorded by the time monitor in the FDTD simulation with the dip at 0.59 THz.

effective optical path length of the THz pulse propagating in the waveguide. The transmission spectrum of the grating is shown in Fig. 5(b). We can observe from the spectrum that the insertion loss for the grating varies from 1 dB to 7 dB between 0.3 and 1 THz. A fine notch of about 23 dB was observed at 0.58 ± 0.01 THz with a line width of ~16 GHz.

#213416 - $15.00 USD Received 3 Jun 2014; revised 12 Aug 2014; accepted 21 Aug 2014; published 8 Sep 2014
(C) 2014 OSA

As the grating consists of non-uniform polymer rods and the spacing between the rods is not equal to its diameter, it is difficult to determine the effective refractive index (n_{eff}) and directly apply the Bragg condition $\lambda_{Bragg} = 2n_{eff}\Lambda$ (where λ_{Bragg} is the reflected wavelength and Λ is the period of the grating). Hence, a commercial-grade simulator based on a finite difference time domain (FDTD) method [31] (where the grating structure can be properly modelled) was used to predict the dip in the transmission spectrum. For the simulation of the grating, the rods were assumed to be regular, featured by a 110 μm diameter and uniformly spaced by 137 μm.

Figure 6(a) displays a snapshot of the FDTD simulation layout. The simulation involved a PML boundary that encloses the simulation area comprising the waveguide, the Bragg grating and the THz single dipole source. A PML provides an index-matching boundary for the simulation region, which thereby prevents the Fresnel reflection of the electromagnetic radiation leaving the simulation region, while avoiding any alteration of the FDTD simulation results from the reflected radiation. For the FDTD simulation the real part of the refractive index of polypropylene was taken to be equal to 1.51 in the range from 0.2 THz to 2.5 THz [32]. The metallic wires were assumed as perfect electric conductors (PECs). The power spectrum from the FDTD simulation predicted the dip in the grating's response to be at ~0.59 THz (Fig. 6(b)) which is in good agreement with the experimental results. However, the dip in case of simulation is ~8 dB as compared to the experimentally observed value of 23 dB. This mismatch in the depth of the dip is most probably due to the simplistic model of our FDTD simulations where the metal wires are assumed as PECs and the loss coefficient of polypropylene is not taken into account.

Acknowledgments

The authors would like to gratefully acknowledge NSERC (the National Science and Engineering Research Council) in Canada and the MESRST (the Ministère de l'Enseignement supérieur, de la Recherche et de la Science et la Technologie) in Quebec. M.C. acknowledges support from the People Program (Marie Curie Actions) of the European Union's Seventh Framework Program (FP7/2007-2013) under the REA grant agreement n° [299522]. M.P. acknowledges the support from the FP7 Marie Curie Actions of the European Commission, via the Career-Integration Grant contract-Nº [630833]. C.R. acknowledges support from a Vanier Canada Graduate Scholarship. M.F. acknowledges support from the People Program (Marie Curie Actions) International Outgoing Fellowship (ATOMIC) under REA grant agreement n° [329346].